RSC Advances

ROYAL SOCIETY OF CHEMISTRY

www.rsc.org/advances

Experimental and Theoretical Evaluation of *trans*-3-Halo-2-Hydroxy-Tetrahydropyran Conformational Preferences. Beyond Anomeric Interaction.

Thaís M. Barbosa[a], Renan, V. Viesser[a], Raymond J. Abraham[b], Roberto Rittner[a]* and Cláudio F. Tormena[a]

[a]*Chemistry Institute, University of Campinas - UNICAMP – P. O. Box: 6154, 13083-970 - Campinas - SP – Brazil. e-mail: rittner@iqm.unicamp.br*

[b]*Department of Chemistry, University of Liverpool – P. O. Box: 147, L69 3BX – Liverpool - UK*

Abstract

Conformational isomerism in *trans*-3-X-2-hydroxy-tetrahydropyrans (X= F, Cl, Br, I) was investigated by NMR spectroscopy and electronic structure calculations. The compounds were synthesized, purified and identified by ^{1}H, ^{13}C and selective TOCSY NMR spectra and by HSQC, COSY and NOESY contour maps. The geometries and conformer energies for the most stable conformers in the isolated molecules were calculated using M06-2X hybrid functional (DFT) and MP2 (*ab initio)* methods with the aug-cc-pVTZ basis set. Theoretical calculations taking into account the solvent effect ($CHCl_3$ and DMSO) were performed using the IEFPCM solvent model, M06-2X/aug-cc-pVTZ level of theory for C, H and O atoms and M06-2X/aug-cc-pVDZ-PP with pseudopotential for the iodine atom. NBO, QTAIM and NCI analyses were applied to identify which stereoelectronic interactions are responsible for their conformational preferences. The conformer stability changes in presence of solvent. The anomeric effect does not appear to have a significant influence on the molecular conformations in these molecules.

Keywords: Tetrahydropyrans; NMR; Conformational analysis; Stereoelectronic interactions.

1. Introduction

The term conformational analysis covers two broad aspects, the determination of the molecular geometry and the conformer energies, followed by studies to determine which stereoelectronic interactions are responsible for the conformational stability.[1] Many detailed studies have investigated the conformational analysis of six-membered rings.[2-8] It has been observed that the most stable conformation of a molecule has a direct dependence on the attractive and repulsive stereoelectronic effects present in the molecular system.[7,9] This may seem obvious, but these effects are not fully understood and many controversies are found in the literature, even for simple systems.[10]

The same controversy is found when dealing with the origin of the anomeric effect. This is a chemical phenomenon that refers to the observed stabilization of an electronegative substituent at C2 in a pyran ring to preferably assume the *axial* position, rather than the equatorial position. However, the real origin of the higher stability of the *axial* conformation of the substituent attached to the anomeric carbon has not been determined so far.[11]

The present study intends to evaluate which are the stereoelectronic interactions responsible for the conformational preferences in *trans*-3-halo-2-hydroxy-tetrahydropyrans (Fig. 1). To assess the stereoelectronic interactions present in these systems it was necessary to analyse the results from NBO (Natural Bond Orbitals)[12], QTAIM (Quantum Theory Atoms in Molecules)[13] and NCI (Non-covalent interactions) topological analyses.[14]

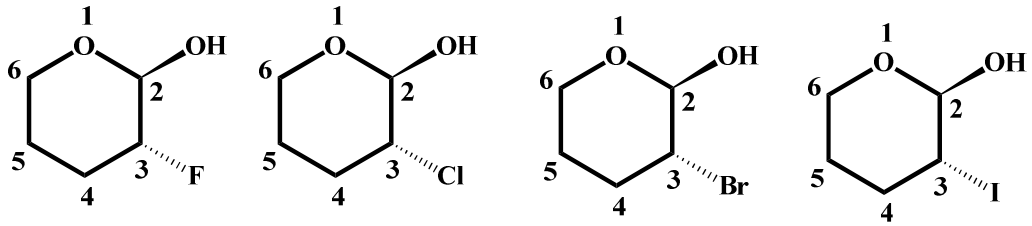

Figure 1: Structure of the studied halohydrins (Halo = F, Cl, Br and I).

2. Experimental section

2.1 Nuclear Magnetic Resonance Experiments

The solvents were commercially available and used without further purification. ^{1}H NMR spectra were recorded on an Avance III spectrometer operating at 600 MHz for ^{1}H. Measurements were carried out at 5 mm TBI probe, at temperature of 25 °C, using solutions about 10 mg cm^{-3} in different solvents. The ^{1}H spectra were referenced to TMS. Typical conditions for the ^{1}H spectra were 8 transients, a spectral width of 4.8 kHz, and 64k data points, giving and acquisition time of 4.5 s. The halohydrins of this study were fully characterized using 1D ^{1}H, ^{13}C and selective TOCSY spectra, as well as, 2D COSY, HSQC and NOESY contour plots.

2.2 Synthesis

It is described the reaction between 3,4-dihydro-2*H*-pyran and the sources of fluorine, chlorine, bromine and iodine (Select-fluor, *N*-chlorosuccinimide, *N*-bromosuccinimide and periodic acid, respectively) leading to diastereoisomeric products, presenting *cis* and *trans* configuration. Both diastereoisomers will be assigned, but only the *trans* product will be discussed in this work. The reaction procedures were adapted according procedure described in literature for similar molecular systems.[15-18]

3-fluoro-2-hydroxytetrahydropyran (1): A solution of nitromethane (50 mL), water (10 mL) and 3,4-dihydro-2*H*-pyran (1.83 mL, 0.02 mol) was cooled at 3 °C and followed by the addition of selectfluor (10 g, 0,03 mol). The reaction was stirred at 25 °C for 12 h. After that, the solution was refluxed (110 °C) for 1 h and concentrated under a reduced pressure to remove the nitromethane. The resulting residue was dissolved in dichloromethane (50 mL), followed by the addition of sodium bicarbonate (5%) solution. The organic layer was washed with brine, dried with magnesium sulfate and concentrated under reduced pressure. The crude product was chromatographed over SiO_2 (70-230 mesh) using a proportion of 7:3 hexane/ethyl acetate as eluent leading to a 41% of yield. Fluorohydrin *cis*: **^{1}H NMR** (600 MHz, $CDCl_3$): δ (ppm) 4.93 (1H, dd, $^3J_{H2H3}$ = 1.98 and $^3J_{H2F}$=10.92 Hz, H2); 4.56 (1H, dddd, $^3J_{H3H4e}$ = 3.06, $^3J_{H3H4a}$ = 7.44 and $^2J_{H3F}$ = 48.43 Hz, H3); 4.02-3.96 (1H, m**,** H6e); 3.59-3.53 (1H, m, H6a); 2.19-2.05 (1H, m, H4e); 1.88-1.78 (2H, m, H4a and H5e) and 1.58-1.49 (1H, m, H5a). **^{13}C NMR** (150 MHz, $CDCl_3$): 92.35 (1C, d, $^2J_{C2F}$ = 19.62 Hz, C2); 87.97 (1C, d, $^1J_{C3F}$ = 178.98 Hz, C3); 62.76 (C6); 25.79 (1C, d, $^2J_{C4F}$ = 20.07 Hz, C4) and 21.63 (1C, d, $^3J_{C5F}$ = 4.53 Hz, C5). Fluorohydrin *trans*: **^{1}H NMR** (600 MHz, $CDCl_3$): δ (ppm) 4.97 (1H, dd, $^3J_{H2H3}$ = 3.72 and $^3J_{H2F}$ = 5.82 Hz, H2); 4.37 (1H, ddt, $^3J_{H3H4e}$ = 3.72, $^3J_{H3H4a}$ = 6.48 and $^2J_{H3F}$ = 48.19 Hz, H3); 4.02-3.96 (1H, m**,** H6e); 3.59-3.53 (1H, m, H6a); 2.19-2.05 (1H, m, H4e); 1.93-1.81 (2H, m, H4a and H5e) and 1.58-1.49 (1H, m, H5a). **^{13}C NMR** (150 MHz, $CDCl_3$): 93.46 (1C, d, $^2J_{C2F}$ = 28.67 Hz, C2); 87.97 (1C, d, $^1J_{C3F}$ = 173.70 Hz, C3); 61.98 (C6); 25.46 (1C, d, $^2J_{C4F}$ = 19.62 Hz, C4) and 21.65 (1C, d, $^3J_{C5F}$ = 4.22 Hz, C5). HRMS EI+ (m/z): Found 120.0589 [M-H$^+$]; C5H9FO2 requires 120.0587 g mol^{-1}.

3-chloro-2-hydroxytetrahydropyran (2): A suspension of *N*-chlorosuccinimide (6.4 g, 0.05 mol) in water (10 mL) was cooled at 3 °C. A solution of 3,4-dihydro-2*H*-pyran (4.34 mL, 0.05 mol) in tetrahydrofuran (20 mL) was added dropwise. The

reaction mixture was stirred for 3 h at 3 °C and concentrated under reduced pressure to remove the tetrahydrofuran. The resulting residue was dissolved in dichloromethane (30 mL), neutralized with a saturated solution of sodium bicarbonate and washed with water. The organic layer was dried with magnesium sulfate and concentrated under reduced pressure. The crude products were chromatographed over SiO_2 (70-230 mesh) using a proportion of 7:3 hexane/ethyl acetate as eluent leading to a 33% of yield. Chlorohydrin *cis*: **^{1}H NMR** (600 MHz, $CDCl_3$): δ (ppm) 4.91 (1H, d, $^3J_{H2H3}$ = 2.04 Hz, H2); 4.13 (1H, ddd, $^3J_{H3H4a}$ = 6.78 and $^3J_{H3H4e}$ = 3.72 Hz, H3); 4.05-4.01 (1H, m, H6e); 3.61-3.55 (1H, m, H6a); 2.24-2.19 (1H, m, H4e); 2.06-2.01 (1H, m, H4a); 1.93-1.81 (1H, m, H5e) and 1.58-1.52 (1H, m, H5a). **^{13}C NMR** (150 MHz, $CDCl_3$): 93.01 (C2); 63.46 (C6); 60.12 (C3); 29.44 (C4) and 22.13 (C5). Chlorohydrin *trans*: **^{1}H NMR** (600 MHz, $CDCl_3$): δ (ppm) 4.79 (1H, d, $^3J_{H2H3}$ = 5.82 Hz, H2); 4.05-4.01 (1H, m, H6e); 3.77 (1H, ddd, $^3J_{H3H4a}$ = 8.58 and $^3J_{H3H4e}$ = 4.32 Hz, H3); 3.61-3.55 (1H, m, H6a); 2.37-2.32 (1H, m, H4e); 1.87-1.81 (2H, m, H4a and H5e) and 1.67-1.59 (1H, m, H5a). **^{13}C NMR** (150 MHz, $CDCl_3$): 97.24 (C2); 64.27 (C6); 58.59 (C3); 30.93 (C4) and 24.09 (C5). HRMS EI+ (m/z): Found 136.0359 [M-H$^+$]; C5H9ClO2 requires 136.0291 g mol^{-1}.

3-bromo-2-hydroxytetrahydropyran (3): A solution of acetone (50 mL) and water (10 mL) was cooled at 10 °C, before the addition of *N*-bromosuccinimide (3.54 g, 0.02 mol) and 3,4-dihydro-2*H*-pyran (1.83 mL, 0.02 mol). The reaction was monitored by the olefin consume by TLC. The reaction mixture was concentrated under reduced pressure to remove acetone and the resulting residue was dissolved in dichloromethane and washed three times with water. The organic layer was dried with sodium sulfate and concentrated under reduced pressure. The crude products were chromatographed over SiO_2 (70-230 mesh) using a proportion of 7:3 hexane/ethyl acetate as eluent leading to a 53% of yield. Bromohydrin *cis*: ^{1}H NMR (600 MHz, $CDCl_3$): δ (ppm) 4.72 (1H, d,

$^{3}J_{H2H3}$ = 1.86 Hz, H2); 4.28 (1H, ddd, $^{3}J_{H3H4a}$ = 6.42 and $^{3}J_{H3H4e}$ = 3.78 Hz, H3); 4.08-4.04 (1H, m, H6e); 3.64-3.57 (1H, m, H6a); 2.35-2.29 (1H, m, H4e); 2.16-2.11 (1H, m, H4a); 2.01-1.89 (1H, m, H5e) and 1.60-1.54 (1H, m, H5a). **^{13}C NMR** (150 MHz, $CDCl_3$): 92.83 (C2); 63.70 (C6); 54.69 (C3); 30.09 (C4) and 22.91 (C5). Bromohydrin *trans*: **^{1}H NMR** (600 MHz, $CDCl_3$): δ (ppm) 4.86 (1H, d, $^{3}J_{H2H3}$ = 6.30 Hz, H2); 4.08-4.04 (1H, m, H6e); 3.88 (1H, ddd, $^{3}J_{H3H4a}$ = 9.60 and $^{3}J_{H3H4e}$ = 4.44 Hz, H3); 3.64-3.57 (1H, m, H6a); 2.46-2.41 (1H, m, H4e); 2.01-1.89 (1H, m, H4a); 1.81-1.76 (1H, m, H5e) and 1.70-1.63 (1H, m, H5a). **^{13}C NMR** (150 MHz, $CDCl_3$): 97.36 (C2); 64.78 (C6); 51.17 (C3); 32.13 (C4) and 25.41 (C5). HRMS EI+ (m/z): Found 161.9682 [M-H^{+}] with the loss of a water molecule; C5H9BrO2 requires 179.9786 g mol^{-1}.

3-iodo-2-hydroxytetrahydropyran (4): To the solution of acetonitrile (40 mL), water (12 mL), 3,4-dihydro-2*H*-pyran (1.83 mL, 0.02 mol) and periodic acid (5.47 g, 24 mmol) was added dropwise (during 2 h) a solution of sodium bisulfite (48 mL, 1 mol L^{-1}). After that, the mixture was stirred for further 2 h at 25 °C. The organic layer was extracted with diethyl ether (300 mL in 3 portions). The organic layer was washed with a saturated solution of sodium sulfite, dried with sodium sulfate and concentrated under reduced pressure. The crude products were chromatographed over SiO_2 (70-230 mesh) using a proportion of 6:4 hexane/ethyl acetate as eluent leading to 18% of yield. Iodohydrin *cis*: ^{1}H NMR (600 MHz, $CDCl_3$): δ (ppm) 4.43 (1H, ddd, $^{3}J_{H3H4a}$ = 6.24, $^{3}J_{H3H4e}$ = 3.72 Hz and $^{3}J_{H3H2}$ =2.10 , H3); 4.15 (1H, d, H2); 4.13-4.05 (1H, m, H6e); 3.66-3.60 (1H, m, H6a); 2.39-2.34 (1H, m, H4e); 2.15-2.08 (1H, m, H4a); 1.92-1.85 (1H, m, H5e) and 1.63-1.56 (1H, m, H5a). **^{13}C NMR** (150 MHz, $CDCl_3$): 93.31 (C2); 63.95 (C6); 37.13 (C3); 31.59 (C4) and 24.29 (C5). Iodohydrin *trans*: **^{1}H NMR** (600 MHz, $CDCl_3$): δ (ppm) 4.90 (1H, d, $^{3}J_{H2H3}$ = 7.08 Hz, H2); 4.13-4.05 (1H, m, H6e); 3.99 (1H, ddd, $^{3}J_{H3H4a}$ = 10.68 and $^{3}J_{H3H4e}$ = 4.44 Hz, H3); 3.66-3.60 (1H, m, H6a); 2.49-2.44

(1H, m, H4e); 2.15-2.08 (1H, m, H4a); 1.72-1.65 (1H, m, H5e) and 1.63-1.56 (1H, m, H5a). **^{13}C NMR** (150 MHz, $CDCl_3$): 98.39 (C2); 65.61 (C6); 34.78 (C4); 30.80 (C3) and 27.27 (C5). HRMS EI+ (m/z): Found 209.9531 [M-H^+] with loss of a water molecule; C5H9IO2 requires 227.9647 g mol^{-1}.

3. Computational details

In the search for the orientation of the O-H group relative to the tetrahydropyran ring, the potential energy curves were scanned using the B3LYP/cc-pVDZ level of theory and varying the C3-C2-O-H dihedral angle from 0 to 360º in 10 degree increments giving 37 possible conformations for each of the four halohydrins studied. For each conformation the C3-C2-O-H dihedral angle was fixed and the rest of the molecule was allowed to relax during the geometry optimization calculations. The geometries for the minima in the curves were then fully optimized at the MP2/aug-cc-pVTZ level of theory available in the Gaussian 09 program.[19] Optimizations were also performed with solvent effect ($CHCl_3$ and DMSO) using the IEFPCM model, M06-2X/aug-cc-pVTZ basis set for C, H and O atoms and M06-2X/aug-cc-pVDZ-PP with pseudopotential for the iodine atom.

Theoretical values for the $^3J_{HH}$ coupling constants were obtained at B3LYP functional (with 25% HF exact-exchange) employing the EPR-III basis set for the hydrogen atom, 6-311G* basis set for the iodine atom and cc-pVDZ basis set for the other atoms using Gaussian 09 program.[19]

Hyperconjugative interactions were evaluated using Natural Bond Orbital (NBO 5.0)[20] analysis as implemented in Gaussian 09, and the calculations were performed at the M06-2X/aug-cc-pVTZ level. QTAIM and NCI topological analyses were performed using the resulting wave functions obtained from the MP2/aug-cc-

pVTZ optimizations. QTAIM and NCI topological analyses were carried out with the AIMALL[21] and NCIPLOT[22] programs, respectively.

4. Results and Discussion

4.1 Experimental results

The reactions between 3,4-dihydro-2*H*-pyran and the sources of fluorine, chlorine, bromine and iodine (Select-fluor, *N*-chlorosuccinimide, *N*-bromosuccinimide and periodic acid, respectively) lead to diastereoisomeric products[23] (see spectra in supporting information), presenting *cis* and *trans* configuration, but the focus of this work was in the *trans* product. Selective TOCSY experiments were performed on all halohydrins under study (see spectra in supporting information) and the ^{1}H signals related to the *trans* diastereoisomer could be selected. Note that the *ax-ax* conformer has both the X and OH substituents in *axial* position, whereas the *eq-eq* conformer has both substituents in *equatorial*. Figure 2 exemplifies the selective TOCSY experiment for the chlorohydrin (**2**).

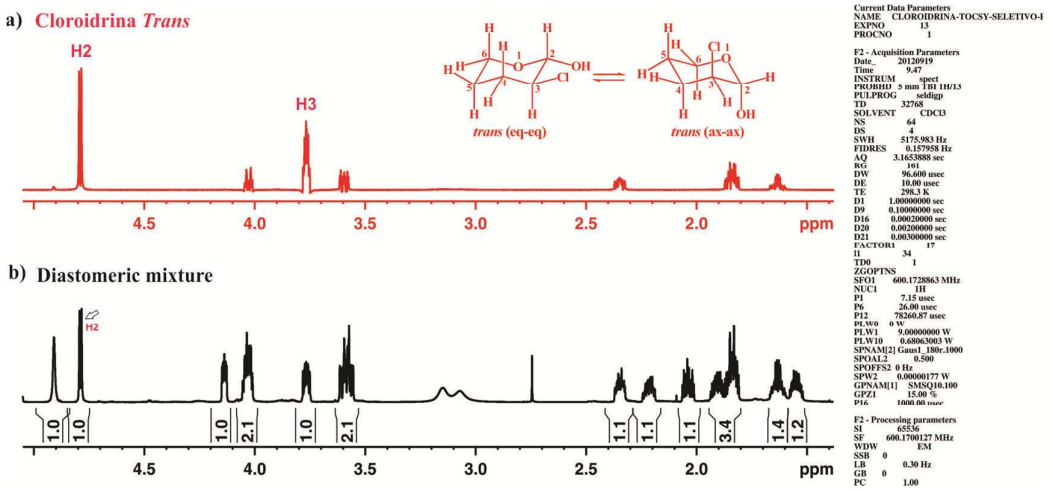

Figure 2: a) Subspectrum of diastereoisomer *trans* of chlorohydrin (**2**) acquired through a selective TOCSY sequence with selection in H2; b) Spectrum of ^{1}H NMR for a mixture of the two diastereoisomers of chlorohydrin (**2**).

The analyses of 1D ^{1}H, ^{13}C and selective TOCSY spectra together with 2D ^{1}H-^{1}H COSY, ^{1}H-^{13}C HSQC and ^{1}H-^{1}H NOESY contour plots were crucial to assign the entire molecule (Table 1).

Table 1: Experimental values of δ_H (ppm) for Fluoro-, Chloro-, Bromo- and Iodohydrin.

	δ_H			
	F	Cl	Br	I
H2	4.97	4.79	4.86	4.90
H3	4.37	3.77	3.88	3.99
H4a	1.93-1.81	1.87-1.81	1.97	2.12
H4e	2.10	2.34	2.43	2.37
H5a	1.52	1.63	1.66	1.59
H5e	1.93-1.81	1.87-1.81	1.78	1.88
H6a	3.57	3.59	3.62	3.64
H6e	4.00	4.03	4.06	4.11

Moreover, the ^{1}H-^{1}H NOESY contour plots suggested that the *trans* diastereoisomers are in conformational equilibrium, since the H2 shows a cross peaks (through space interaction) with H6a, H4a and H3, as exemplified for the chlorohydrin (Fig. 3). This conclusion comes from the observed correlation between H2 with H4a and H6a, which is expected to appear only in the *eq-eq* conformation, whereas the correlation between H3 and H2 is expected to appear only in the *ax-ax* conformation.

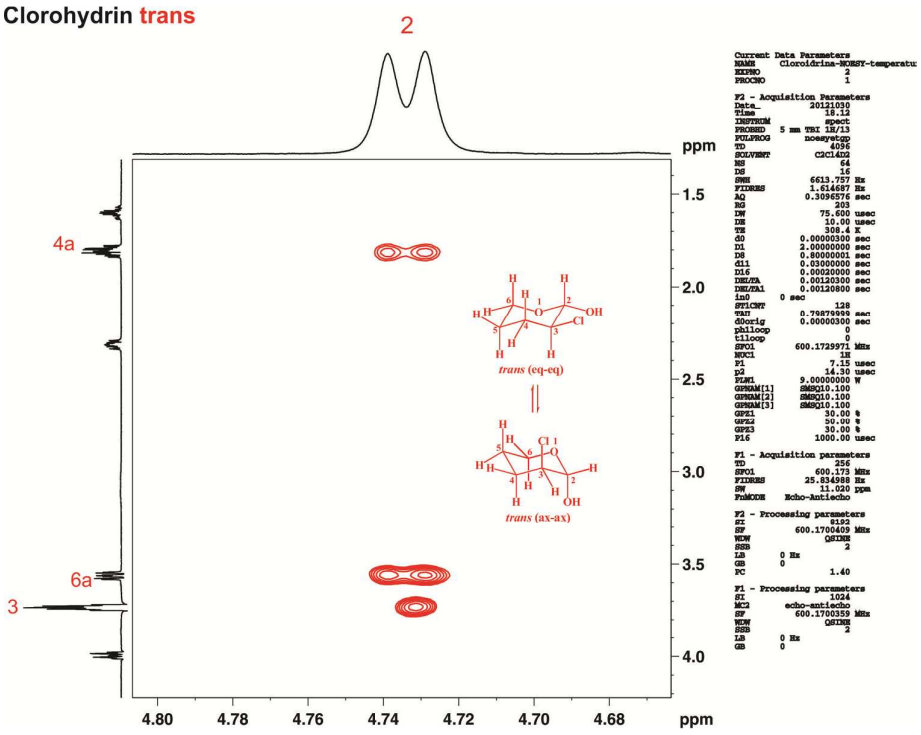

Figure 3: The conformational equilibrium observed for the *trans* chlorohydrin (**2**).

To evaluate the conformational equilibrium, ^{1}H NMR spectra for compounds **1-4** were acquired in solvents of different permittivity constant (dielectric constant), and the vicinal $^{3}J_{H3H2,}$ $^{3}J_{H3H4a}$ and $^{3}J_{H3H4e}$ coupling constants were measured straightforwardly from the H3 signal, which is a first-order spin system (Table 2). The solvents used were $CDCl_3$, $C_2D_2Cl_4$, acetone-d_6, CD_3CN and DMSO-d_6.

Table 2: Coupling constants *J* (Hz) of H3 measured in solvents with different polarity.

Halogen	^3J	$CDCl_3$	$C_2D_2Cl_4$	Acetone-d_6	CD_3CN	DMSO-d_6
Fluoro	H3H2	3.72	4.08	3.84	3.96	4.14
	H3H4e	3.72	4.08	3.84	4.50	4.14
	H3H4a	**6.48**	**6.84**	**6.54**	**6.60**	**6.78**
Chloro	H3H2	5.82	6.12	5.64	6.18	6.06
	H3H4e	4.32	4.32	4.26	4.32	4.32
	H3H4a	**8.58**	**8.94**	**8.34**	**9.24**	**9.18**
Bromo	H3H2	6.30	6.54	6.12	6.66	6.48
	H3H4e	4.44	4.44	4.32	4.44	4.38
	H3H4a	**9.60**	**9.90**	**9.36**	**10.02**	**9.78**
Iodo	H3H2	7.08	7.26	6.96	7.26	7.20
	H3H4e	4.44	4.44	4.38	4.44	4.38
	H3H4a	**10.68**	**10.98**	**10.38**	**11.34**	**10.74**

In the analyses of the observed coupling constant values, it has to be taken into account that they are averaged values of the conformers that participate in the conformational equilibrium. The data from Table 2 suggests the preference for the *eq-eq* conformer increases from fluorine to iodine derivatives, since $^3J_{H3H4a}$ changes from 6 Hz to 11 Hz. Also $^3J_{H3H4a}$ for each halogen shows only small changes for all solvents used (Table 2), suggesting that solvent polarity does not appreciably affect the conformational equilibrium. These results indicate that the conformation equilibrium for studied compounds is dictated by halogen, instead of solvent polarity.

4.2 Computational results

In order to analyse the stability of the *trans* halohydrins a potential energy curve was acquired at the B3LYP level using cc-pVDZ basis set varying the C3-C2-O-H dihedral angle from 0° to 360° in 10° increments (Fig. 4).

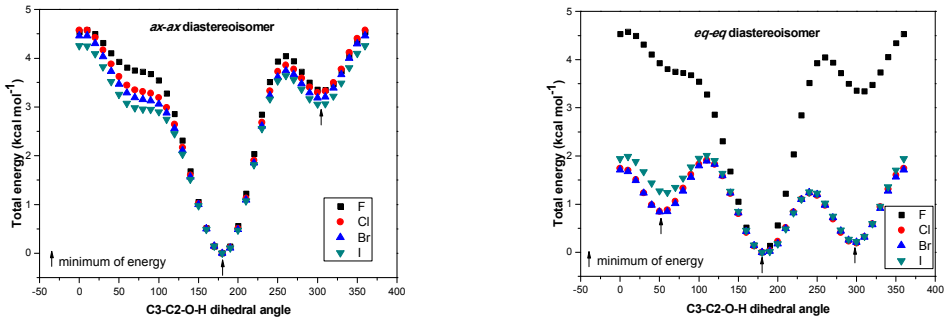

Figure 4: The potential energy curves for the *trans* halohydrins **1**-**4**.

The potential energy curves (Fig. 4) provide the angles and structures for the most stable conformers for each compound. The geometry for each local minimum was re-optimized at the MP2/aug-cc-pVTZ level and the results of the most stable conformer or the minimum global of energy, that is always the dihedral angle of 180º, are summarized in Table 3.

Table 3: Electronic energies for the most stable conformer of each halohydrins with ZPE correction, applying MP2 approximation and aug-cc-pVTZ basis set for C, H and O atoms and aug-cc-pVDZ-PP with pseudopotential for the iodine atom.

Halohydrins	Energy[a]	ΔE (*eq-eq* - *ax-ax*)[b]
F-*ax-ax*	-445.36572	0.0
F-*eq-eq*	-445.36323	1.6
Cl-*ax-ax*	-805.35373	0.0
Cl-*eq-eq*	-805.35232	0.9
Br-*ax-ax*	-2918.34220	0.0
Br-*eq-eq*	-2918.34090	0.8
I-*ax-ax*	-640.43731	0.0
I-*eq-eq*	-640.43657	0.5

[a] In a.u. where 1 a.u. = 627.509 kcal mol^{-1}; [b] kcal mol^{-1}

The energy values showed in Table 3 are related to the energy of the isolated molecule in vapour phase. Through these calculations the *ax-ax* conformer is more stable than the *eq-eq* by 1.6, 0.9, 0.8 and 0.5 kcal mol^{-1} for the fluorohydrin, chorohydrin, bromohydrin and iodohydrin, respectively.

The main stereoeletronic interactions responsible for the stability of the *ax-ax* conformer in the vapour phase of each compound under study were evaluated through NBO, QTAIM and NCI analyses. The NBO with deletion and NBO steric analysis gave the results showed in Table 4. The NBO steric analysis give a result that is similar to the concept of steric "contact" between occupied orbitals.

Table 4: Variations of the total energy (ΔE) in vapor phase (MP2/aug-cc-pVTZ), the steric energy from the NBO-steric (ΔE st) and of the hyperconjugative energy from the NBO-del (ΔE hyper) and the dipole moment (μ).

Halohydrins	ΔE [a]	ΔE st [a]	ΔE hyper [a]	μ [b]
F-*ax-ax*	0.0	1.6	0.0	2.05
F-*eq-eq*	1.6	0.0	-2.4	3.35
Cl-*ax-ax*	0.0	4.0	0.0	2.26
Cl-*eq-eq*	0.9	0.0	-4.6	3.44
Br-*ax-ax*	0.0	3.2	0.0	2.33
Br-*eq-eq*	0.8	0.0	-4.6	3.47
I-*ax-ax*	0.0	6.3	0.0	2.25
I-*eq-eq*	0.5	0.0	-4.6	3.35

[a)] in kcal mol^{-1}; [b)] μ in debye (D).

The first analysis from Tables 3 and 4 shows that the energy variation between the *ax-ax* and *eq-eq* conformers decreases in the order F>Cl>Br>I. These data indicate

that the halogen size is related to the conformer stability as mentioned before. The steric repulsion energy (ΔE st) increases from fluorohydrin to iodohydrin leading to a destabilization of the *ax-ax* conformer.

However, it was not possible to appoint a specific repulsive interaction responsible for this effect since the observed result is due to the sum of all interactions. Thus, considering that the halogen size is involved in the conformational behavior the interaction involving a halogen can be used to explain the observed results. In this way the interactions between $\sigma_{C3\text{-}X} \rightarrow \sigma_{C2O2}$ and $\sigma_{C3\text{-}X} \rightarrow \sigma_{C4H4a}$ are depicted in Figure 5 and their energies are listed in Table 5.

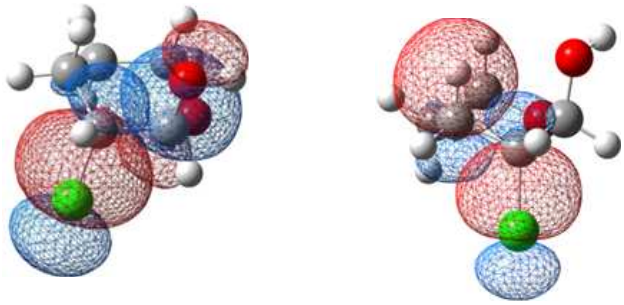

Figure 5: Representation of $\sigma_{C3\text{-}Cl} \rightarrow \sigma_{C2\text{-}O2}$ and $\sigma_{C3\text{-}Cl} \rightarrow \sigma_{C4H4a}$ repulsion interaction for the *ax-ax* chlorohydrin **(2)**, respectively.

Table 5: Repulsive interactions energies (σ→σ), in kcal mol^{-1}, for fluoro- chloro-, bromo- and iodohydrin for the *ax-ax* conformation.

Interaction	F	Cl	Br	I
$\sigma_{C3\text{-}X} \rightarrow \sigma_{C2O2}$	1.0	3.8	4.3	5.2
$\sigma_{C3\text{-}X} \rightarrow \sigma_{C4H4a}$	1.2	5.8	6.4	6.8

Table 4 also lists the hyperconjugative interaction energies (ΔE hyper) obtained from NBO analysis, where it is shown that the *eq-eq* conformer is more stabilized by this kind of interaction. Thus, both steric and hyperconjugative energy interactions should yield a destabilization of *ax-ax* conformer, but this conformer shows the lowest energy. At this stage, non-covalent interactions can be invoked to explain the stabilization of *ax-ax* conformer.

However, which atoms should be involved in this stabilization? The isosurfaces provided by the NCI topology (Fig. 6) show that an interaction between the oxygen lone pairs from OH group and the H4 and H6 in *axial* orientation, as well as, the halogens lone pair with the H5 in *axial* orientation are responsible for the *ax-ax* stabilization.

It is important to highlight that hydrogen bond O—H---X is not present among the stabilizing interactions, since, theoretically analyses (NBO, NCI and QTAIM) did not show any evidence of its existence. A recent investigation[24] compares the chemical shifts of the OH proton in $DMSO$ *vs* $CDCl_3$ to predict hydrogen bond formation through Equation 1. When A < 0.1 there is intramolecular hydrogen bond formation. The value of A for the studied compounds was 0.5 which does not represent a hydrogen bond and this agrees with the above theoretical data.

$$A = 0.0065 + 0.133\Delta\delta \quad (1)$$

$$\Delta\delta = \delta(DMSO) - \delta(CDCl3)$$

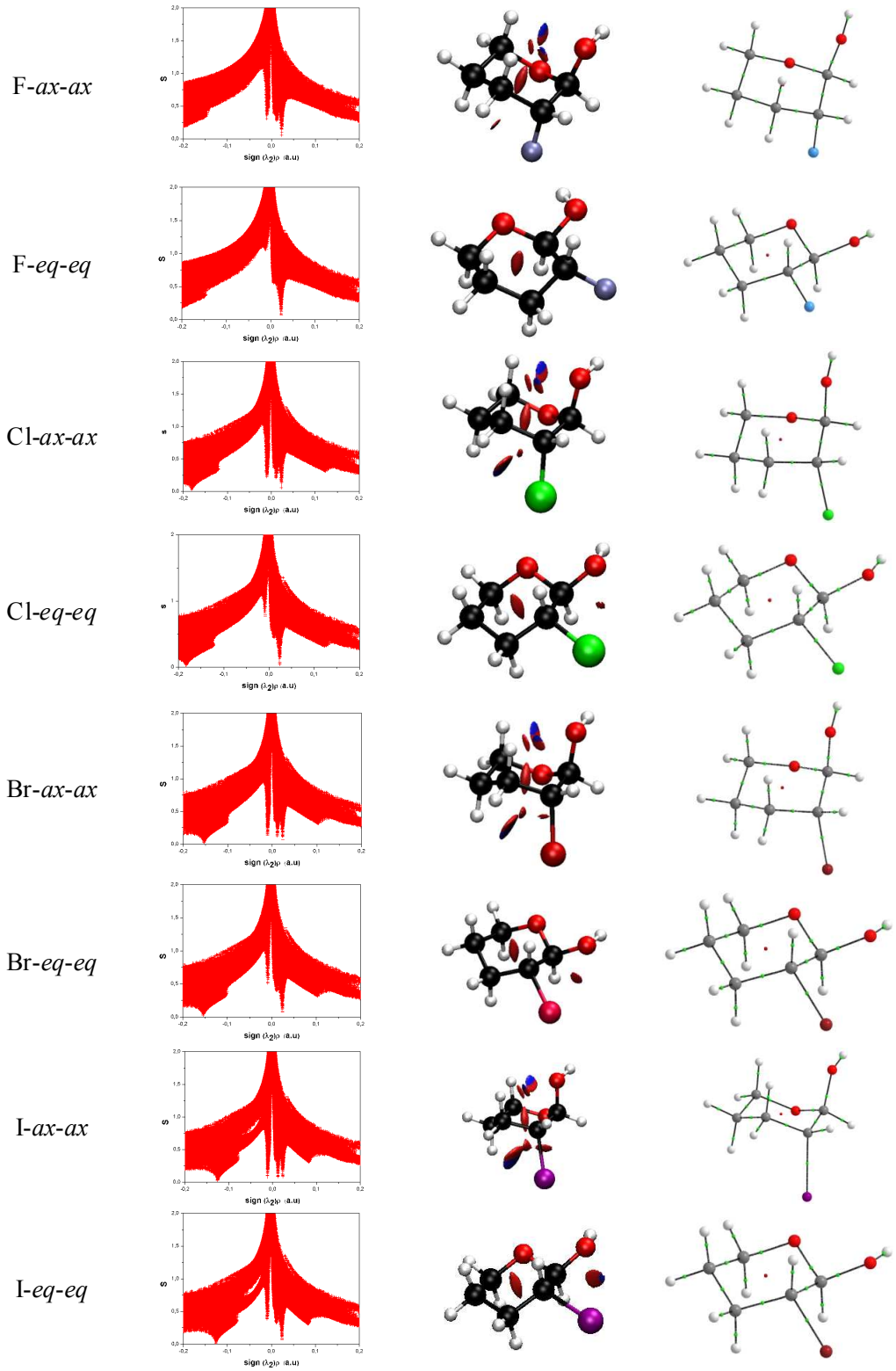

Figure 6: Plot of the reduced density gradient **s** and sign(λ2)ρ; NCI isosurfaces and QTAIM image, respectively, for the compounds **1-4**.

It is important to highlight that the graphics of reduced density gradients (Fig. 6) are similar in shape among *ax-ax* conformers and among *eq-eq* conformers for the halohydrins. It has been observed negative values for λ_2 in RDG, indicating an attractive interaction in the NCI plot (Fig. 6) for the *ax-ax* and *eq-eq* conformers, however for the *ax-ax* conformer it is observed a higher intensity, resulting in a blue interaction in the NCI surfaces. These attractive interactions are not observed in the QTAIM image as a bond critical point (BCP), since the reduced density gradient (s) does not achieve (touch) the zero value.

The stabilization of the *ax-ax* conformer is due to the non-covalent interactions present in the vapour phase. However in solution these interactions are reduced or vanish due to solvation which is proportional to the conformer dipole moment. This may explain why the values of the observed coupling constants ($^3J_{H3H4a}$) increase from fluorine to iodine from 6 Hz to 11 Hz (Table 2), which can only be due to the preference for the *eq-eq* conformer. To confirm this idea, theoretical calculations, taking into account the solvent effect ($CHCl_3$ and DMSO), were performed and the results are showed in Figure 7.

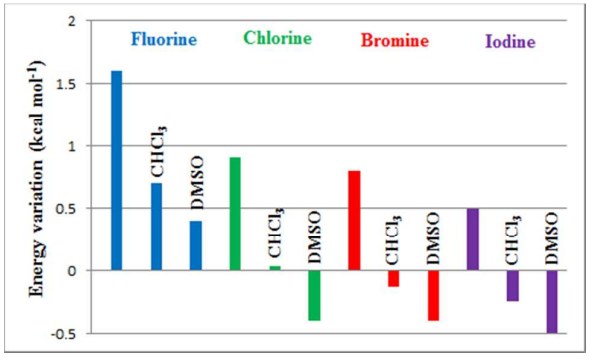

Figure 7: Graphic representing the theoretical energy of *eq-eq* conformer in relation to the *ax-ax* conformer for all halohydrins without and with solvent effect ($CHCl_3$ and DMSO - IEFPCM). All calculations were performed with M06-2X level of theory.

Theoretical calculations with solvent effect were fundamental to prove the influence of solvent in conformer's stability. For all halohydrins the solvent favored the *eq-eq* conformer, for the fluorohydrin the stabilization of *ax-ax* conformer was 1.5 kcal mol^{-1} in vapor phase and this value was reduced to 0.5 kcal mol^{-1} when the solvent effect (DMSO) was included, whereas, for chloro-, bromo- and iodohydrin the *eq-eq* became more stable. The conformers energies taking into account the solvent effect explain the percentage obtained experimentally for the halohydrins (Table 6).

Table 6: Percentage of *ax-ax* conformer in the equilibrium obtained through theory (Equation 2) and coupling constant $^{3}J_{H3H4a}$ (Equation 3).

Solvent		Fluorohydrin	Chlorohydrin	Bromohydrin	Iodohydrin
		ax-ax	*ax-ax*	*ax-ax*	*ax-ax*
DMSO-d_6	Eq. 2	68%	35%	33%	30%
	Eq. 3	60%	37%	35%	25%
$CDCl_3$	Eq. 2	76%	51%	45%	39%
	Eq. 3	63%	43%	37%	26%

The proportion of the isomers (Table 6) present in the conformational equilibrium was calculated through the Equation 2 (Boltzmann equation) and Equation 3.

$$\frac{\eta_x}{\eta_y} = e^{\frac{-\Delta E}{K_B T}} \quad (2)$$

Where, η represents the molar fraction of a specific conformer; ΔE the energy variation between them; K_B the Boltzmann constant and T the temperature (298 K); *x* represents the *ax-ax* conformer and *y* the *eq-eq* conformer.

NMR at low temperatures (-80 ºC) were performed in order to determine the proportion of each conformer in the equilibrium, however even at low temperatures was not possible to separate the signals of each conformer. Equation 3 was used to this propose.

$$J_{obs} = \eta_x J_x + \eta_y J_y \qquad (3)$$

$$\eta_x + \eta_y = 1$$

J_{obs} is the observed experimental coupling constant; η the molar fraction of a specific conformer; *J* is the calculated coupling constant of each isomer isolated (Table 7); *x* represents the *ax-ax* conformer and *y* the *eq-eq* conformer.

Table 7: Values of coupling constant (*J*) in Hz of each isomer isolated obtained at B3LYP/EPR-III for the hydrogen atoms.

	Fluorohydrin		Chlorohydrin		Bromohydrin		Iodohydrin	
	ax-ax	eq-eq	ax-ax	eq-eq	ax-ax	eq-eq	ax-ax	eq-eq
$^5J_{H3H2}$	1.91	7.07	1.75	7.96	2.02	8.51	1.48	8.66
$^3J_{H3H4e}$	**3.51**	6.42	**3.18**	5.97	**3.48**	6.27	**3.03**	5.77
$^3J_{H3H4a}$	3.09	**11.51**	4.35	**12.65**	4.83	**13.22**	4.69	**13.30**

Also a prevalence of the *ax-ax* conformation would be expected due to the anomeric effect, because for halohydrins under study the R-X-CH2-Z fragment, where

X is an electronegative atom and Z is usually an oxygen, is present. Usually, molecules with this fragment are stabilized by a specific orbital interaction delocalization, dubbed anomeric effect.[11a] However, many controversies are found in the literature related to the real origin of anomeric effect. Some authors suggest that it is due to an electrostatic interaction, while others ascribe it to hyperconjugation involved in anomeric effect (Fig. 8).[11]

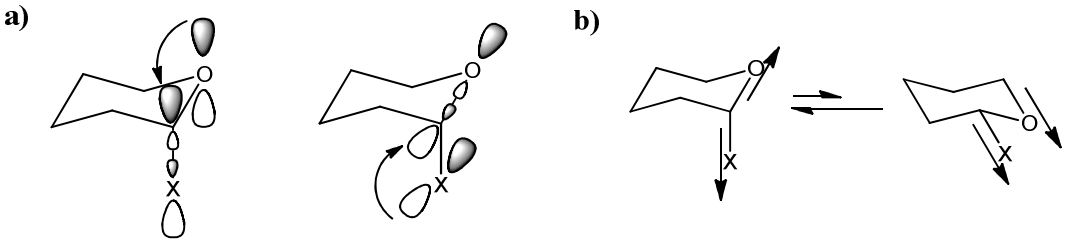

Figure 8: a) Orbital interactions known as *endo*- and *exo*-anomeric effect respectively; b) dipole moments for the two conformers; X represents the oxygen of the molecules under study.

Table 8 shows the energy values related to the *endo*- and *exo*-anomeric effect for the halohydrins under study (Fig. 1).

Table 8: Hyperconjugation energy values for *trans* diastereoisomers (kcal mol^{-1}).

Halohydrins	$LP1_{O1} \rightarrow *\sigma_{C2\text{-}O2}$ *endo*	$LP2_{O1} \rightarrow *\sigma_{C2\text{-}O2}$ *endo*	$LP2_{O2} \rightarrow *\sigma_{C2\text{-}O1}$ *exo*
F-*ax*-*ax*	-1.1	-16.5	-14.0
F-*eq*-*eq*	-4.2	-	-14.8
Cl-*ax*-*ax*	-1.2	-16.6	-13.7
Cl-*eq*-*eq*	-4.6	-	-13.7
Br-*ax*-*ax*	-1.1	-16.7	-13.8
Br-*eq*-*eq*	-4.7	-	-13.4
I-*ax*-*ax*	-1.2	-16.3	-13.9
I-*eq*-*eq*	-4.3	-	-13.1

The values shown in Table 8 suggest that the *ax*-*ax* conformer is more stabilized by the anomeric effect, presenting a high value for both the *endo*- and the *exo*-anomeric effects. However, it is important to remember that in the sum of all hyperconjugative interactions the *eq*-*eq* conformers have higher hyperconjugative interactions than the *ax*-*ax* conformers (Table 4). Thus, for the halohydrins under study the anomeric effect has no prevalence in the conformational stabilization.

5. Conclusion

The higher stability of the *ax*-*ax* conformer in isolated phase is due to strong non-covalent interactions. However these interactions are minimized in solution leading to a higher proportion of the *eq*-*eq* conformer in the presence of solvent. In this way, the theoretical and experimental data are in agreement. The anomeric effect does not appear to be fundamental to explain the stability of these molecules.

Acknowledgment

The authors thank a grant #2014/25903-6 and #2013/03477-2 São Paulo Research Foundation (FAPESP), for providing financial support for this research, for scholarships [to T.M.B. #2014/12776-6; R.V.V.#2012/12414, FAPESP) and also the CNPq for fellowships (to R.R. #300379/2009-9 and C.F.T. #302095/2013-6), and the Chemistry Institute of UNICAMP for the facilities.

References

1 D. S. Ribeiro and R. Rittner, *J. Org. Chem.,* 2003, **68**, 6780-6787.

2 F. Yoshinaga, C. F. Tormena, M. P. Freitas, R. Rittner and R. J. Abraham, *J. Chem. Soc. Perkin Trans. 2*, 2002, 1494-1498.

3 F. P. dos Santos and C. F. Tormena, *J. Mol. Struct. THEOCHEM*, 2006, **763**, 145-148.

4 P. R. Anizelli, J. D. Vilcachagua, A. Cunha Neto and C. F. Tormena, *J. Phys. Chem. A*, 2008, **112**, 8785-8789.

5 M. P. Freitas, C. F. Tormena and R. Rittner, *J. Mol. Struct.*, 2001, **570**, 175-180.

6 M. P. Freitas, C. F. Tormena, R. Rittner and R. J. Abraham, *J. Phys. Chem.,* 2003, **16**, 27-33.

7 M. P. Freitas, R. Rittner, C. F. Tormena and R. J. Abraham, *Spectrochim. Acta A*, 2005, **61**, 1771-1776.

8 M. L. Senent, A. Niño, C. Muñoz-Caro, Y. G. Smeyers, R. Domínguez-Gómez and J. M. Orza, *J. Phys. Chem. A*, 2002, **106**, 10673-10680.

9 F. Cortes-Gusman, J. Hernandez-Trujillo and G. Cuevas, *J. Phys. Chem. A*, 2003, **107**, 9253-9256.

10 a) V. Pophristic and L. Goodman, *Nature*, 2001, **411**, 565-568; b) P. R. Schreiner, *Angew. Chem. Int. Ed.*, 2002, **41**, 3579-3581; c) F. M. Bickelhaupt and E. J.

Baerends, *Angew. Chem. Int. Ed.*, 2003, **42**, 4183-4188; d) L. Goodman, H. Gu and V. Pophristic, *J. Phys. Chem. A*, 2005, **109**, 1223-1229; e) Y. Mo and J. Gao, *Acc. Chem. Res.*, 2007, **40**, 113-119; f) S. Liu and N. Govind, *J. Phys. Chem. A*, 2008, **112**, 6690-6699; g) R. A. Cormanich and M. P. Freitas, *J. Org. Chem.,* 2009, **74**, 8384-8387.

11 a) E. J. Cocinero, P. Çarçabal, T. D. Vaden, J. P. Simons and B. G. Davis, *Nature*, 2011, **469**, 76-79; b) Y. Huang, A-G. Zhong, Q. Yang and S. Liu, *J. Chem. Phys.*, 2011, **134**, 84103; c) Y. Mo, *Nature Chem.*, 2010, **2**, 666-671.

12 F. Weinhold, *J. Comp. Chem.*, 2012, **33**, 2363-2379.

13 R. F. W. Bader, Atoms in Molecules A Quantum Theory, Clarendon press, Oxford, **1994**.

14 E. R. Johnson, S. Keinan, P. Mori-Sánchez, J. Contreras-García, A. J. Cohen and W. Yang, *J. Am. Chem. Soc.*, 2010, **132**, 6498–6506.

15 I. Fokt, S. Szymanski, S. Skora, M. Cybulski, T. Madden and W. Priebe, *Carbohydrate Research*, 2009, **344**, 1464-1473.

16 Jeong-Seok Chae, and col., U. S. Pat. Appl. Publ., 14 Aug 2003.

17 B. K. Bettadaiah, K. N. Gurudutt and P. Srinivas, *J. Org. Chem.*, 2003, **68**, 2460-2462.

18 H. Masuda, K. Takase, M. Nishio, A. Hasegawa, Y. Nishiyama and Y. Ishii, *J. Org. Chem.*, 1994, **59**, 5550-5555.

19 Gaussian 09, Revision **D.01**, M. J. Frisch, G. W. Trucks, H. B. Schlegel, G. E. Scuseria, M. A. Robb, J. R. Cheeseman, G. Scalmani, V. Barone, B. Mennucci, G. A. Petersson, H. Nakatsuji, M. Caricato, X. Li, H. P. Hratchian, A. F. Izmaylov, J. Bloino, G. Zheng, J. L. Sonnenberg, M. Hada, M. Ehara, K. Toyota, R. Fukuda, J. Hasegawa, M. Ishida, T. Nakajima, Y. Honda, O. Kitao, H. Nakai, T. Vreven, J. A.

Montgomery, Jr., J. E. Peralta, F. Ogliaro, M. Bearpark, J. J. Heyd, E. Brothers, K. N. Kudin, V. N. Staroverov, R. Kobayashi, J. Normand, K. Raghavachari, A. Rendell, J. C. Burant, S. S. Iyengar, J. Tomasi, M. Cossi, N. Rega, J. M. Millam, M. Klene, J. E. Knox, J. B. Cross, V. Bakken, C. Adamo, J. Jaramillo, R. Gomperts, R. E. Stratmann, O. Yazyev, A. J. Austin, R. Cammi, C. Pomelli, J. W. Ochterski, R. L. Martin, K. Morokuma, V. G. Zakrzewski, G. A. Voth, P. Salvador, J. J. Dannenberg, S. Dapprich, A. D. Daniels, Ö. Farkas, J. B. Foresman, J. V. Ortiz, J. Cioslowski, and D. J. Fox, Gaussian, Inc., Wallingford CT, 2009.

20 E. D. J. Glendening, K. Badenhoop, A. E. Reed, J. E. Carpenter, J. A. Bohmann, C. M. Morales and F. Weinhold, *NBO 5.0.*, Theoretical Chemistry Institute, University of Wisconsin, Madison (2001).

21 T. A. Keith, AIMALL, version 11.10.16; TK Gristmill Software: Overland Park, KS, 2011. aim.tkgristmill.com.

22 a) J. Contreras-García, E. R. Johnson, S. Keinan, R. Chaudret, J. P. Piquemal, D. N. Beratan and W. Yang, *J. Chem. Theory Comput*., 2011, **7**, 625−632; b) E. R. Johnson, S. Keinan, P. Mori-Sanchez, J. Contreras-Garcia, A. J. Cohen, W. Yang, *J. Am. Chem. Soc*., 2010, **132**, 6498-6506.

23 R. U. Lemieux and B. Fraser-Reid, *Can. J. Chem*., 1965, **43**, 1460-1475.

24 M. H. Abraham, R. J. Abraham, W. E. Acree, Jr., A. E. Aliev, A. J. Leo and W. L. Whaley, *J. Org. Chem*, 2014, **79**, 11075-83.